Canadian Science Publishing

INVITED REVIEW

Methods to identify and characterize iron–sulfur oligopeptides in water

Luca Valer, Daniele Rossetto, Simone Scintilla, Yin Juan Hu, Anju Tomar, Serge Nader, Isaiah O. Betinol, and Sheref S. Mansy

Abstract: Iron–sulfur clusters are ubiquitous cofactors that mediate central biological processes. However, despite their long history, these metallocofactors remain challenging to investigate when coordinated to small (≤ six amino acids) oligopeptides in aqueous solution. In addition to being often unstable in vitro, iron–sulfur clusters can be found in a wide variety of forms with varied characteristics, which makes it difficult to easily discern what is in solution. This difficulty is compounded by the dynamics of iron–sulfur peptides, which frequently coordinate multiple types of clusters simultaneously. To aid investigations of such complex samples, a summary of data from multiple techniques used to characterize both iron–sulfur proteins and peptides is provided. Although not all spectroscopic techniques are equally insightful, it is possible to use several, readily available methods to gain insight into the complex composition of aqueous solutions of iron–sulfur peptides.

Key words: iron–sulfur cluster, metallopeptide, prebiotic chemistry, origins of life.

Résumé : Les agrégats fer-soufre sont des cofacteurs omniprésents qui interviennent dans les processus biologiques centraux. Cependant, malgré leur longue histoire, ces métallofacteurs restent difficiles à étudier lorsqu'ils sont coordonnés à de petits oligopeptides (≤ six acides aminés) en solution aqueuse. En plus d'être souvent instables in vitro, les agrégats fer-soufre peuvent exister dans une grande variété de formes aux caractéristiques diverses, ce qui complique l'identification des différentes formes en solution. Cette difficulté est amplifiée par la dynamique des peptides fer–soufre, qui se coordonnent souvent à plusieurs types d'agrégats en même temps. Pour faciliter les recherches sur ces échantillons complexes, nous présentons un résumé des données issues de plusieurs techniques utilisées pour caractériser les protéines et les peptides fer-soufre. Bien que toutes les techniques spectroscopiques n'offrent pas le même niveau de pertinence, il est possible d'utiliser plusieurs méthodes facilement accessibles pour mieux comprendre la composition complexe de solutions aqueuses de peptides fer-soufre. [Traduit par la Rédaction]

Mots-clés : agrégat fer–soufre, métallopeptide, chimie prébiotique, origines de la vie.

Introduction

All living organisms are reliant on metal ions for structure, signal transduction, and catalysis. This dependence on metal ions must reflect the environments from which life evolved and likely emerged.[1] While individual biological molecules can be engineered[2] and can evolve away from metal-dependent function,[3,4] large scale reorganization leading to decreased reliance on metal ions appears to be inhibited by a lack of selective pressure for some metal ions and the pervasiveness, and thus entrenchment, of some metallocofactors throughout central metabolism. An illustration of the latter is the continued cellular dependence on iron ions despite the transition from an anoxygenic, iron-rich environment to an oxygenated planet with iron concentrations many fold lower.[1] This continued dependence on iron ions has led to the speculation that the metal mediated cellular chemistry observed today reflects the types of reactions that were needed by the first protocellular systems that emerged on our planet. That is, evolution harnessed what was there from the beginning by providing scaffolds that fine-tuned the intrinsic reactivity of available metal ions.[5,6]

Iron is the most abundant transition metal of our universe, our planet, and of extant biology. Therefore, prebiotic chemistry on the early Earth must have been influenced by the iron that was present. Attempts at delineating abiotic reaction networks similar to contemporary metabolism have frequently relied on the presence of iron ions,[7,8] although alternative scenarios have been described.[9–11] Early enzymes may have more frequently exploited iron ions than genomic analyses indicate, as some modern day enzymes that make use of other divalent cations may have coordinated Fe^{2+} in the past.[4,12] However, the same redox properties that make iron a versatile and powerful catalyst also make this metal ion toxic to modern organisms, if not properly regulated. Indeed, contemporary organisms go through great lengths to

Received 22 August 2021. Accepted 12 December 2021.

L. Valer, D. Rossetto, S. Scintilla, and A. Tomar. Department CIBIO, University of Trento, Via Sommarive 9, Povo, TN 38123, Italy.
Y.J. Hu, S. Nader, and I.O. Betinol. Department of Chemistry, University of Alberta, 11227 Saskatchewan Drive, Edmonton AB T6G 2G2, Canada.
S.S. Mansy. Department CIBIO, University of Trento, Via Sommarive 9, Povo, TN 38123, Italy; Department of Chemistry, University of Alberta, 11227 Saskatchewan Drive, Edmonton AB T6G 2G2, Canada.

Corresponding author: Sheref Mansy (email: sheref.mansy@ualberta.ca).

This paper is part of a special issue dedicated to the careers of Professors Jed Harrison, Charles Lucy, and Richard McCreery of the Department of Chemistry at the University of Alberta.

Fig. 1. Different types of iron–sulfur clusters commonly found in biology. $[2Fe\text{-}2S]^0$, $[4Fe\text{-}4S]^0$, and $[4Fe\text{-}4S]^{4+}$ clusters do not typically form. An expanded version that includes [3Fe-4S] clusters is provided as Supplementary Fig. S1. The clusters can also be represented in their anionic form as $(RS)_4[1Fe\text{-}0S]^{2-/1-}$, ferredoxin $(RS)_4[2Fe\text{-}2S]^{3-/2-}$, Rieske $(RS)_2[2Fe\text{-}2S]^{1-/0}$, and $(RS)_4[4Fe\text{-}4\ S]^{3-/2-/1-}$. [Colour online.]

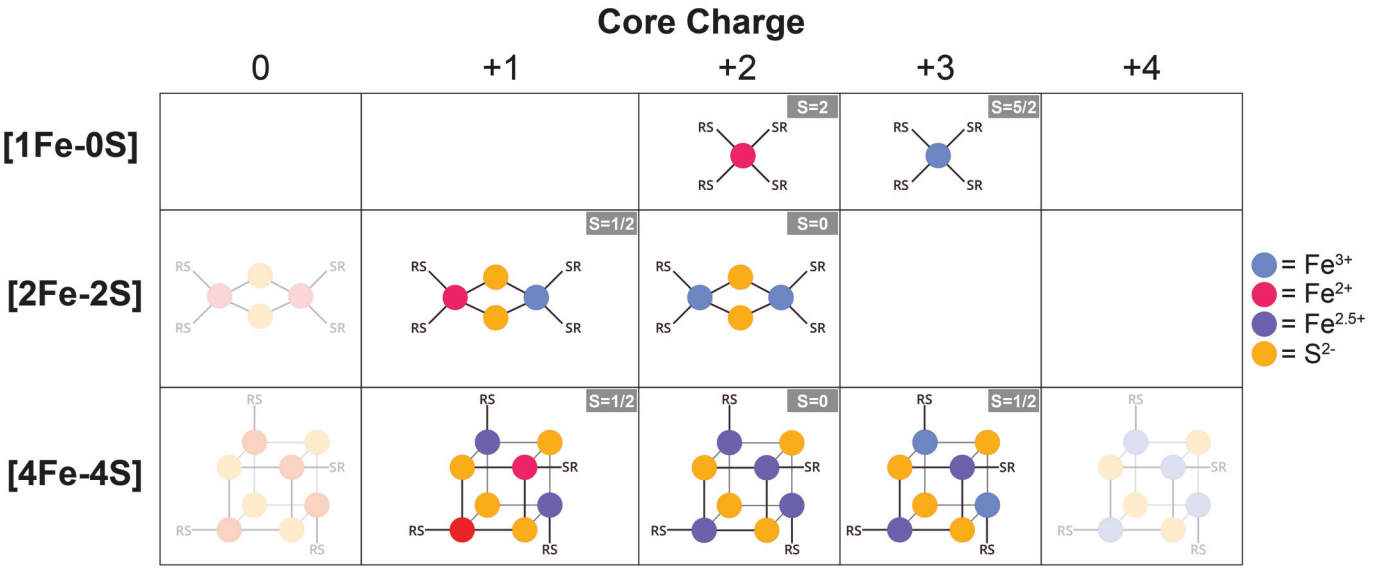

traffic iron ions so as to avoid Fenton-like reactions that can damage proteins, DNA, and lipids.[13–16]

One subset of iron proteins almost universally found in biology is iron–sulfur proteins. The most common iron–sulfur clusters include [1Fe-0S], [2Fe-2S], and [4Fe-4S] clusters where the iron centres are typically tetrahedrally coordinated by the thiolate sidechains of cysteines (Fig. 1). Polynuclear iron–sulfur clusters are additionally coordinated by acid labile, bridging sulfides.[17] Although protein ligation is typically provided by cysteine residues, there are several examples of non-cysteinyl ligands. For example, Rieske-like clusters are [2Fe-2S] clusters in which one iron ion is coordinated by two cysteines and the other iron center is coordinated by two histidines.[18] Another example is the enzyme aconitase, which coordinates a [4Fe-4S] cluster with three cysteines. The open coordination sphere is either occupied by solvent or substrate.[19] [1Fe-0S] and [2Fe-2S] clusters are typically found in biology in two different oxidation states, i.e., $[1Fe\text{-}0S]^{3+/2+}$ and $[2Fe\text{-}2S]^{2+/+}$. Although not thought to be physiologically relevant, $[2Fe\text{-}2S]^0$ clusters can be formed in dimethylformamide and acetonitrile.[20,21] [4Fe-4S] proteins can be divided into two categories, low potential and high potential. Low potential iron–sulfur proteins contain a $[4Fe\text{-}4S]^{2+/+}$ cluster, and high potential iron–sulfur proteins possess a $[4F\text{-}4S]^{3+/2+}$ cluster. Reduction potentials are strongly influenced by their coordination sphere within the polypeptide.[22] A $[4Fe\text{-}4S]^0$ cluster can sometimes be obtained through the use of strong reducing agents, but this all-ferrous form is not thought to exist in biology.[23]

Contemporary iron–sulfur proteins catalyze a wide range of reactions inside the cell and play a particularly prominent role in electron transfer.[24] Additionally, iron–sulfur clusters can act as Lewis acids, as seen with the unique, non-cysteinyl ligated iron centre of aconitase.[19] Iron–sulfur proteins can additionally donate sulfur, provide structural stability, assemble cofactors, and sense the metallation status of the cell.[25] Because of their ubiquity, role in central metabolism, evolutionary conservation, and the ease with which iron–sulfur clusters assemble in vitro, iron–sulfur clusters are frequently referred to as ancient.[26,27] Tellingly, examples of abiotic, metabolic-like pathways that proceed in the presence of either metallic iron or iron ions have had difficulty mediating reactions reliant on iron–sulfur clusters in biology.[8,28] Such difficulties may indicate a need for simple, prebiotically plausible iron–sulfur cluster catalysts, perhaps similar to the short iron–sulfur peptides described thus far.[29–32]

Iron–sulfur clusters have been abiotically synthesized in the laboratory since at least the 1970s.[26] Frequently, these early studies made use of non-biological scaffolds and biologically inspired, termini-protected cysteine-containing peptides in organic solvents, such as methanol, tetrahydrofuran, or acetonitrile.[33] The data from these model systems revealed the requirements and mechanisms for the synthesis of iron–sulfur clusters and aided efforts to characterize the geometry, stability, magnetism, reduction potential, ligand exchange rates, and reactivity of a variety of clusters.[26] More recently, iron–sulfur peptides have been synthesized in aqueous solution. For example, the Cowan group synthesized a [2Fe-2S] cluster coordinated to the tripeptide L-glutathione (γECG) in water.[34] Later work showed that iron–sulfur clusters could be stabilized in aqueous solution by the vast majority of cysteine-containing tripeptides and that UV light facilitates the synthesis of [2Fe-2S] and [4Fe-4S] clusters by providing the necessary inorganic ingredients.[29] Duplications of the glutathione sequence into hexa- and dodeca-peptides increase the stability of the cluster in water, suggesting that a modified Eck–Dayhoff-like scenario[5,31,35] may have been possible where a protoferredoxin may have emerged from the accretion of smaller peptides.[29,36]

The synthesis of longer iron–sulfur peptides frequently exploits motifs found in nature. For example, the ferredoxin maquette FdM from the Dutton group exploits a $CX_3CX_2CX_2C$ motif based on the [4Fe-4S] cluster binding pocket of *Peptococcus aerogenes* ferredoxin I;[37] however, the need for β-mercaptoethanol suggests that one of the cysteines may not ligate the cluster. This motif possesses a CX_2C sequence that is extremely common in biology and likely is central for cluster loading and stability for [1Fe-0S], [2Fe-2S], and [4Fe-4S] clusters.[38] Frequently, three of the cysteine ligands are close in primary sequence with a more distant fourth cysteine. Alternatively, two different two cysteine-containing motifs can be found in which all four cysteines together bind a single [1Fe-0S] or [2Fe-2S] cluster.[37] Other motifs that have been used to synthesize iron–sulfur peptides include $CX_2CX_2CX_2C$ for ferredoxin-like sequences[29,31] and radical SAM-inspired motifs that contain only three cysteines, such as CX_2CX_2C and CX_3CX_2C.[39] What makes investigating scaffolds that do not provide four thiolate ligands to the cluster (e.g., hexapeptides or shorter that only contain one or two Cys) difficult to

Fig. 2. Spectra of aqueous mixtures of iron–sulfur clusters stabilized by glutathione (γECG). (A) Spectra are of $[1Fe\text{-}0S]^{2+}$ GCPLCG (blue), $[2Fe\text{-}2S]^{2+}$ PESCKAGACSTCAGPDLTCT (red), and $[4Fe\text{-}4S]^{2+}$ KLCEGGCIACGACGGW (yellow). All spectra arise from the mixing of 1.25 mM peptide, 0.4 mM Fe^{3+}, and 50 mM Gly-Gly at pH 8.7. The conditions for $[2Fe\text{-}2S]^{2+}$ PESCKAGACSTCAGPDLTCT and $[4Fe\text{-}4S]^{2+}$ KLCEGGCIACGACGGW also contained 0.19 mM and 0.8 mM hydrosulfide (HS^-), respectively. Further, the conditions for the $[4Fe\text{-}4S]^{2+}$ peptide included 2% (v/v) β-mercaptoethanol. Spectra were plotted from previously published data,[40] and the raw data are available at Zenodo.[50] (B) UV–vis spectrum of 40 mM glutathione, 0.5 mM Na_2S, and 0.5 mM $FeCl_3$ at pH 8.6, which contained a mixture of types of iron–sulfur clusters. (C) Paramagnetic ^1H NMR spectrum of a similar sample (150 mM glutathione, 1.88 mM Na_2S, and 1.88 mM $FeCl_3$ at pH 8.6) revealed the presence of $[1Fe\text{-}0S]^{2+}$, $[2Fe\text{-}2S]^{2+}$, and $[4Fe\text{-}4S]^{2+}$ clusters at 210 ppm (blue), 33 ppm (red), and 11.8 ppm (yellow), respectively. [Colour online.]

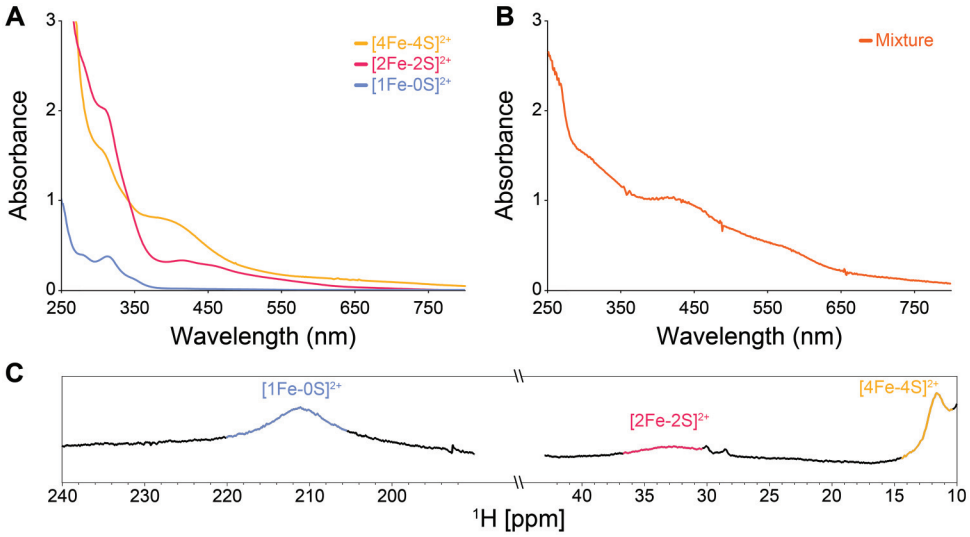

characterize is that the same peptide can bind different types of iron–sulfur clusters at the same time. For example, it is not unusual for small (≤6 amino acids) peptides to stabilize the formation of a mixture of [1Fe-0S], [2Fe-2S], and [4Fe-4S] clusters in aqueous solution, with the relative ratios reflecting the amount of hydrosulfide present.[30] Because of the complicated electronic transitions and the variability in extinction coefficients of the different types of iron–sulfur clusters, deciphering what is present can be challenging. Therefore, it is important to collect and compare data with multiple techniques. To facilitate efforts in characterizing iron–sulfur peptides, we have attempted to provide here a brief compilation of published data on short peptides in organic solvent and aqueous solution along with representative examples of iron–sulfur proteins. The main spectroscopic features of UV–vis absorption, circular dichroism, resonance Raman, paramagnetic NMR, EPR, and Mössbauer spectroscopies, in addition to measurements of reduction potentials are provided and reveal the similarities and differences between different types of iron–sulfur clusters.

UV–vis absorption spectroscopy

UV–vis spectroscopy is the easiest and most accessible technique to characterize iron–sulfur peptides. Spectrophotometers are inexpensive, and the acquisition of spectra is quick. The difficulty lies with the fact that there is much overlap in spectral features, which can make quantitative analysis of mixtures difficult. Spectral decomposition programs can help to identify the types of clusters present in aqueous solution. Recently, an easy-to-use Microsoft Excel based spectral decomposition tool was made freely available.[40] Generally, iron–sulfur clusters absorb in the 300–800 nm range, reflecting the LMCT (ligand-to-metal charge transfer) transitions (Fig. 2A).[41] The simplest iron–sulfur complex found in proteins is that of rubredoxin, which is why [1Fe-0S] complexes are frequently referred to as rubredoxin-like centres. For such [1Fe-0S] complexes, these bands correspond to Fe (3*d*) ← S-Cys (*n*). For comparison, the UV–vis spectra of oxidized $[1Fe\text{-}0S]^{3+}$ rubredoxin show several peaks between 350 nm and 380 nm, with a maximum absorbance at ∼490 nm and a broad band centered near 560 nm.[42,43] The extinction coefficient of [1Fe-0 S]$^{3+}$ rubredoxin at 490 nm is ∼7000 M^{-1} cm^{-1}.[40] Small (≤6 amino acids) $[1Fe\text{-}0S]^{3+}$ peptides rarely show similar spectra to the rubredoxin protein. Instead, a single broad band at ∼490 nm is typically observed.[44,45] The reduced $[1Fe\text{-}0S]^{2+}$ state for both rubredoxin and peptides show much less spectral features, with a main peak centered near 310 nm and a shoulder at 350 nm (Supplementary Table S1).[46–49]

$[2Fe\text{-}2S]^{2+}$ clusters give the most distinctive UV–vis spectra that are remarkably similar between full-length proteins and peptides.[28] The bands at approximately 420 and 450 nm, mainly attributable to Fe (3*d*) ← μ-S (*n*) electronic transitions in the visible region,[50] are the most diagnostic for the presence of a $[2Fe\text{-}2S]^{2+}$ cluster,[51–55] although there are also bands at 330 nm and occasionally a discernable broad band between 550 and 600 nm. The extinction coefficient of $[2Fe\text{-}2S]^{2+}$ ferredoxin at 420 nm is ∼11 000 M^{-1} cm^{-1}.[55] The $[2Fe\text{-}2S]^{2+}$ cluster of Rieske proteins with two Cys and two His ligands show bands at 460 and 490 nm.[18,56] Spectra of $[2Fe\text{-}2S]^{+}$ clusters are generally less featured, with a single broad band at 410 nm (Supplementary Table S2).

$[4Fe\text{-}4S]^{2+}$ clusters typically show a broad band between 400 and 420 nm both in low potential proteins[57–63] and synthetic analogues.[36,38,58,64–68] The extinction coefficient of $[4Fe\text{-}4S]^{2+}$ ferredoxin at 390 nm is ∼17 000 M^{-1} cm^{-1}.[58] High-potential iron–sulfur proteins (i.e., HiPIP) with a $[4Fe\text{-}4S]^{2+}$ cluster are similar, showing a broad band in the range of 380–420 nm. $[4Fe\text{-}4S]^{+}$ clusters are typically characterized by the absence of any distinctive absorption band in the visible region,[69,70] whereas $[4Fe\text{-}4S]^{3+}$ clusters display a red-shifted broad band at ∼450 nm flanked by a broad band at 320 nm (Supplementary Table S3).[71]

Circular dichroism spectroscopy

The environment surrounding an iron–sulfur cluster within a protein is asymmetric, which can be exploited by circular dichroism (CD) spectroscopy to gain some insight into the type of cluster present (Supplementary Table S4).[47–49] Such spectra are collected

in the near-UV and visible regions, probing the same electronic transitions seen when collecting absorption spectra as described above.[73,74] Although there is much variability in what is observed by CD spectroscopy, CD spectra do not require labeled nor high concentrations of sample and are easy to acquire. Further, free metal ions do not give rise to interfering absorbance, since $[Fe(H_2O)_6]^{2+}$, for example, is achiral.[75] CD spectra of $[2Fe\text{-}2S]^{2+}$ and $[4Fe\text{-}4S]^{2+}$clusters tend to both show two clear positive bands near 450 nm and 550 nm.[75,76] The $[1Fe\text{-}0S]^{3+}$ of rubredoxin also has a positive band near 450 nm but a negative band near 550 nm.[75] However, given that CD spectra are greatly impacted by geometry and symmetry, spectra can look different in wavelength and intensity for the same cluster type coordinated to different proteins. CD spectroscopy can also be used to confirm ligand substitution. For example, the visible CD spectra of $[2Fe\text{-}2S]^{2+}$ Rieske proteins (2 Cys and 2 His ligands) show a prominent negative band at 370 nm, which is not seen for adrenodoxin (4 Cys ligands).[56] This makes CD spectroscopy useful in monitoring the transfer of cluster from one protein to another.[77] Conversely, iron–sulfur clusters coordinated to small peptides are often spectroscopically silent by CD or display weak CD bands. The lack of CD spectra indicates a symmetric environment around the iron–sulfur cluster.[78] Taken together, CD is a quick and useful method to characterize iron–sulfur proteins but is generally more useful for monitoring perturbations to the cluster environment or reactions over time as opposed to providing convincing evidence of cluster type. A similar, complementary technique is magnetic circular dichroism (MCD), which incorporates a magnetic field to help distinguish between overlapping electronic transitions. Despite being superior to absorption and non-magnetic circular dichroism,[73,79] MCD spectrometers are not readily available to typical laboratories.

Resonance Raman spectroscopy

Resonance Raman (RR) spectroscopy is a powerful tool for the identification and characterization of metal sites and the elucidation of structure–function relationships of metalloproteins and metallopeptides. RR spectroscopy is particularly insightful when investigating iron–sulfur clusters that are diamagnetic and thus EPR silent (e.g., $[2Fe\text{-}2S]^{2+}$ and $[4Fe\text{-}4S]^{2+}$ clusters). Incident light that excites the Fe ← S charge transfer electronic transitions (LMCT) enhances spectra manyfold, greatly facilitating spectral acquisition. For this reason, the wavelength of excitation often matches the characteristic spectral features of the cluster species. Commonly used excitation wavelengths are 406 nm, 458 nm, and 496 nm. The resulting spectra are sensitive to the configuration, symmetry, nature of ligands, and ultimately the type of iron–sulfur cluster present (Supplementary Table S5).[80,81]

RR spectra of ferric rubredoxin ($[1Fe\text{-}0S]^{3+}$, but not $[1Fe\text{-}0S]^{2+}$, is RR active) show a characteristic, but not necessarily resolved, four-line pattern in the 310–380 cm^{-1} range, which originate from Fe–S stretching modes that involve mostly symmetric and asymmetric changes of the lengths of the four Fe–S(Cys) bonds. The most intense band, found at ca. 315 cm^{-1}, is attributed to a totally symmetric breathing mode of the FeS_4 tetrahedron. Bands of significantly lower intensities, centred at ∼360 cm^{-1}, originate from triply degenerate asymmetric Fe–S stretching.[82]

[2Fe-2S] clusters are usually RR active as $[2Fe\text{-}2S]^{2+}$ and less frequently as $[2Fe\text{-}2S]^{+}$. Generally, the RR spectra of $[2Fe\text{-}2S]^{2+}$ ferredoxins are more complex and more informative than RR spectra of rubredoxin. For $[2Fe\text{-}2S]^{2+}$ clusters, the predominant mode is found near 290 cm^{-1} for a cluster completely coordinated by cysteines. Two additional, well-resolved modes are found within 320–340 cm^{-1} and (or) at 390–400 cm^{-1}.[83] $[2Fe\text{-}2S]^{+}$ clusters show bands of similar relative intensities as for $[2Fe\text{-}2S]^{2+}$ clusters but are shifted to lower frequencies by 15–40 cm^{-1}.[84] Rieske iron–sulfur clusters are Raman active as $[2Fe\text{-}2S]^{2+}$. Because of the lower symmetry of the cluster, RR spectra of Rieske proteins have a higher number of bands in the 200–450 cm^{-1} region than their $[2Fe\text{-}2S]^{2+}$ ferredoxin-like counterparts.[85]

$[4Fe\text{-}4S]^{2+}$ clusters are Raman active. For all cysteinyl-coordinated $[4Fe\text{-}4S]^{2+}$ clusters, the most intense band falls in the 330–340 cm^{-1} range. The terminal modes are found at approximately 360 cm^{-1} and 390 cm^{-1}.[86] The HiPIPs contain a $[4Fe\text{-}4S]^{3+/2+}$ cluster and both are Raman active. As seen for low potential $[4Fe\text{-}4S]^{2+}$ clusters, RR spectra of $[4Fe\text{-}4S]^{3+}$ HiPIP are dominated by the totally symmetric bridging vibration of the cluster core, which is found within the 340–345 cm^{-1} region. RR spectra of reduced $[4Fe\text{-}4S]^{2+}$ HiPIP are quite similar to spectra of oxidized $[4Fe\text{-}4S]^{3+}$ HiPIP with the most intense band lying at ca. 335 cm^{-1}.[68]

Paramagnetic NMR spectroscopy

The history of paramagnetic NMR is longer than often appreciated with spectra of cytochrome c and a non-heme iron protein published in 1965 and 1977, respectively.[43,87] Insightful reviews on the use of paramagnetic NMR for the study of iron–sulfur proteins have been previously published.[88,89] Unlike many of the techniques used to interrogate iron–sulfur clusters, paramagnetic NMR can typically observe iron–sulfur clusters at all of their oxidation states and can be acquired at room temperature. Unpaired electrons possess a magnetic moment ∼600 fold greater than the magnetic moment of a proton, which significantly influences the surrounding nuclei, with broadening observed with a $1/r^6$ dependence from the metal centre.[90] Depending on the rate of electronic relaxation of the paramagnetic centre, nearby nuclei may either be quenched or shifted, with the latter giving rise to what is known as hyperfine shifted resonances. In the case of iron–sulfur clusters, the presence of the paramagnetic core will considerably influence the resonances of surrounding nuclei, particularly the protons of ligating cysteines and NH groups involved in HN–S interactions.[91,92] Paramagnetic NMR is described in greater depth here more than the other techniques, because most laboratories have easy access to NMR spectrometers.

$[1Fe\text{-}0S]^{3+}$ rubredoxin contains a single ferric ion with $S = 5/2$. The fast relaxation occurring in the presence of this high spin metal ion strongly influences both the hyperfine shift of the resonances and their linewidths. Cys H_α nuclei are typically easily observed within the 10–20 ppm region (Supplementary Table S6).[93,94] However, the detection of the Cys H_β is more difficult. Broadening is often significant enough to make the Cys H_β resonances unobservable. However, when the Cys H_β resonances are seen, the resonances fall within the 100–300 ppm range. Better spectra may be obtained by deuterium NMR with $^2H_\beta$-Cys-labelled proteins, which may allow for the detection of all the Cys H_β signals between 300 and 700 ppm. It is difficult to observe $[1Fe\text{-}0S]^{3+}$ coordinated to small peptides, because the iron ion is frequently reduced to Fe^{2+} with concomitant oxidation of non-ligating cysteines.[29] The $[1Fe\text{-}0S]^{2+}$ state of the protein rubredoxin possesses a single ferrous ion with $S = 2$. This high-spin metal ion still induces considerable downfield hyperfine shifts of Cys H_β resonances (in the 180–250 ppm region) but with significantly sharper signals with respect to that of the $[1Fe\text{-}0S]^{3+}$. Resonances of Cys H_α may be observed between 10–20 ppm and –20–0 ppm. Paramagnetic ^1H spectra of $[1Fe\text{-}0S]^{2+}$ peptides are characterized by similar signals in polar organic solvents, such as acetonitrile and dimethylsulfoxide (DMSO), and water suggesting negligible solvent effects on the cluster core with respect to proteins (Supplementary Fig. S2*a*).[49,95] The spectra are in general consistent with those of Fe^{2+}, which have shorter electronic relaxation times and better resolved ^1H NMR resonances in comparison with Fe^{3+} species.[49,93]

$[2Fe\text{-}2S]^{2+}$ clusters contain two antiferromagnetically coupled Fe^{3+} ions that give rise to a S = 0 ground state. Due to coupling, the resulting H_β resonances of ligating cysteines in ferredoxins are found much more upfield (between 20 and 40 ppm) and are broader with respect to what is found for $[1Fe\text{-}0S]^{3+}$. In addition, the H_α resonances fall in the diamagnetic envelope for some

ferredoxins.[96,97] [2Fe-2S] Rieske clusters display a similar broad resonance between 20 and 40 ppm as seen with ferredoxins (Supplementary Fig. S2*b*).[95] The shift of the Cys H_β resonances of spectra of reduced $[2Fe\text{-}2S]^+$ ferredoxins are more variable. When reduction leads to a mixed valence cluster, i.e., a $[2Fe\text{-}2S]^+$ cluster containing one ferric and one ferrous ion, the resonances are sharper[98,99] than when the additional electron is delocalized over both iron ions, i.e., when the cluster contains two $Fe^{2.5+}$. In the first case, the sharp resonances are localized upfield, in the region from –15 to 45 ppm, and downfield in the 80–140 ppm range.[56,100] In the second case, the CH_β resonances are broader and sometimes below the limit of detection. $[2Fe\text{-}2S]^{2+}$ peptides display hyperfine shifts similar to $[2Fe\text{-}2S]^{2+}$ proteins (Supplementary Fig. S2*b*).[53–55] However, few examples of $[2Fe\text{-}2S]^+$ peptides characterized by NMR have been reported. One example is of a 20 amino acid peptide with a $[2Fe\text{-}2S]^+$ cluster that exhibited broad proton resonances of the ligating cysteines in the 10–40 ppm region.[54]

$[4Fe\text{-}4S]^{2+}$ clusters are the most frequently encountered form of [4Fe-4S] clusters and contain two identical, valence delocalized, $Fe^{2.5}$–$Fe^{2.5+}$ pairs that are antiferromagnetically coupled with a $S = 0$ ground state. $[4Fe\text{-}4S]^{2+}$ proteins exhibit hyperfine resonances of Cys H_β in a narrow range between 10 and 20 ppm.[101,102] Upon reduction to $[4Fe\text{-}4S]^+$, the obtained $S = 1/2$ ground state can be described as the antiferromagnetically coupling of a mixed valence $Fe^{2.5+}$–$Fe^{2.5+}$ pair with a purely ferrous pair, Fe^{2+}–Fe^{2+}, with associated hyperfine resonances spread over a wider 10–60 ppm range.[100,103,104] The less common $[4Fe\text{-}4S]^{3+}$ HiPIPs give the clearest paramagnetic NMR spectra with sharp, well-resolved resonances appearing within 40 to 90 ppm.[105] The spectral improvement is the result of larger magnetic couplings among the iron ions and thus shorter electron spin relaxation times in comparison with $[4Fe\text{-}4S]^{2+}$ and $[4Fe\text{-}4S]^+$ clusters.[89] There are several published examples of paramagnetic NMR spectra of $[4Fe\text{-}4S]^{2+}$ peptides. The spectra are similar to spectra of $[4Fe\text{-}4S]^{2+}$ proteins, with Cys H_β resonances shifted to 0–20 ppm (Supplementary Fig. S2*c*).[65,66,106–108] Conversely, only one example of $[4Fe\text{-}4S]^+$ peptide spectra is reported. This dodecapeptide coordinates the iron–sulfur cluster with four Cys residues that show α and β proton resonances between 10 and 75 ppm.[30] Paramagnetic ^1H spectroscopy has been used to decipher solutions containing a mixture of different types of iron–sulfur clusters in organic solvent[109] and aqueous solution (Figs. 2B and 2C). Such equilibria have also been quantified by Mössbauer spectroscopy.[29]

EPR spectroscopy

Just as for NMR spectroscopy, electron paramagnetic resonance (EPR) spectroscopy exploits the presence of a magnetic moment (electronic, in this case) immersed in an external magnetic field, that interacts with an electromagnetic frequency.[110] Briefly, EPR-active molecules possess one or more unpaired electrons. Detected signals are affected by their chemical environment and are reported relative to the frequency of a free unpaired electron (g_e). Different than NMR spectroscopy, EPR acquisitions require much higher frequency (microwaves) and low working temperatures as the relaxation times are much faster. Therefore, with a solid sample, g is composed of three spatial components depending on the orientation of the dipole with respect to the applied magnetic field, whose entity depends on the symmetry of the electronic distribution in the molecule. Similar to paramagnetic NMR spectroscopy, the interaction between an unpaired electron and the nuclear magnetic moment (i.e., the electron-nuclear hyperfine interaction) provides information on the molecule. Differently than NMR spectroscopy, nuclear–nuclear spin interactions are negligible in EPR. On the contrary, the electron–electron coupling in the presence of more unpaired electrons can differently affect the signals depending on the strength of the interaction (antiferromagnetic/ferromagnetic coupling or spin-correlated electronic couples in case of strong or weak electron–electron coupling, respectively).

Continuous wave (CW) and pulsed EPR spectroscopy are possible. In CW EPR, an electromagnetic frequency continuously irradiates the sample, and resonances are generated by sweeping the magnetic field over a specific range. As a result, only the electron-nuclear hyperfine couplings are observed, and spectra are presented as derivatives. CW is the most common EPR technique. In pulsed EPR experiments, more similarly to NMR spectroscopy, the sample is irradiated by electromagnetic pulses. However, differently than in NMR spectroscopy, the magnetic field could be kept fixed or varied, depending on the desired investigation, providing information on specific interactions in detail. Electron–nuclear double resonance (ENDOR) and hyperfine sublevel correlation (HYSCORE) are typical pulse EPR experiments.[110] Signal fitting is usually required for a correct interpretation of the EPR spectra, with many tools available for this purpose.[111]

The presence of unpaired electrons within an iron–sulfur cluster makes EPR spectroscopy perfectly suitable for the interrogation of the cluster. However, unlike paramagnetic NMR spectroscopy, only iron–sulfur clusters with an S integer ($S = 1, 2, \ldots n$) or half-integer are EPR active. Anti-ferromagnetic spin coupling in $[2Fe\text{-}2S]^{2+}$ and $[4Fe\text{-}4S]^{2+}$ make these clusters EPR silent ($S = 0$). Conversely, their reduced forms, i.e., $[2Fe\text{-}2S]^+$ and $[4Fe\text{-}4S]^+$, are EPR active with $S = 1/2$. EPR spectra of $[1Fe\text{-}0S]^{3+}$ rubredoxins isolated from different organisms typically report signals at $g = 4.3$ and $g = 9.7$ (Supplementary Table S7), assigned to excited and ground state transitions, respectively.[112–115] However, different values have been recorded despite the $[1Fe\text{-}0S]^{3+}$ complex existing in the same oxidation state and geometry, demonstrating the impact of the chemical environment on EPR spectra.[116] Although high-spin ($S = 2$) ferrous ion is paramagnetic, EPR studies of this ion coordinated to peptides and small molecules are notably problematic. Often the resulting $[1Fe\text{-}0S]^{2+}$ is reported as EPR silent.[113,115] Frozen aqueous solutions of ferrous complexes with β-mercaptoethanol, dithiothreitol, and the tripeptide glutathione exhibit a signal at $g = 10$ that is assigned to a pseudo-tetrahedral geometry.[117,118] However, Knapp et al. used high frequency EPR spectroscopy to show g values for mononuclear, non-peptidyl Fe^{2+} analogues in organic solvent ($g_x = g_y = 2.08$, $g_z = 2.00$).[119]

Polynuclear clusters, when they are not EPR silent, generally show g values near 1.94. For example, $[2Fe\text{-}2S]^+$ ferredoxins ($S = 1/2$) exhibit EPR resonances with typical average g values near 1.94,[55,120] and EPR spectra of $[2Fe\text{-}2S]^+$ Rieske proteins have a g value of approximately 1.9.[121] Different types of ferredoxins can be distinguished by three g values, including plant-type ($g_1 = 1.88$, $g_2 = 1.96$, $g_3 = 2.05$), vertebrate-type ($g_1 = 1.94$, $g_2 = 1.94$, $g_3 = 2.02$), and bacterial-type ($g_1 = 1.92$, $g_2 = 1.94$, $g_3 = 2.00$) ferredoxins.[52] Similar values are observed for non-proteinaceous $[2Fe\text{-}2S]^+$ clusters stabilized by bulky synthetic ligands or a 20 amino acid peptide in aqueous solution.[54,122] A $[2Fe\text{-}2S]^+$ cluster coordinated by a peptide with a CX_2C motif showed EPR spectra with average g values near $g \approx 1.94$. However, $[2Fe\text{-}2S]^+$ peptides frequently show signs of decomposition at $g = 4$, consistent with either reductively lability or reductive coupling to form an EPR silent $[4Fe\text{-}4S]^{2+}$ cluster.[53] Interestingly, $[2Fe\text{-}2S]^{1+}$ clusters typically exhibit slow relaxation, resulting in non-significant broadening at 70 K.[23]

[4Fe-4S] clusters have been extensively characterized by EPR spectroscopy. [4Fe-4S] clusters are EPR active in the low-potential reduced $[4Fe\text{-}4S]^+$ state and in the high-potential oxidized $[4Fe\text{-}4\ S]^{3+}$ state, both having $S = 1/2$. $[4Fe\text{-}4S]^+$ clusters tend to give more consistent spectra with typical average g values near 1.96.[66,123] Protein bound $[4Fe\text{-}4S]^{3+}$ clusters are more variable but show an average g value of 2.01,[124,125] plus additional features indicative of heterogeneity.[68,69] A $[4Fe\text{-}4S]^+$ dodecapeptide with four cysteine ligands to the cluster gave EPR spectra similar to that of a $[4Fe\text{-}4S]^+$ protein, as shown by simulations with $g_1 = 2.0445$, $g_2 = 1.9365$, and $g_3 = 1.903$.[30]

Fig. 3. Mössbauer spectroscopy of iron–sulfur peptides. (A) Typical Mössbauer spectral parameters of common iron–sulfur clusters. (B) Mössbauer spectrum of Fe^{2+} coordinated by glutathione (100 mol% Fe^{2+}). (C) Mössbauer spectrum of a mixture of $[1Fe\text{-}0S]^{2+}$ and $[2Fe\text{-}2S]^{2+}$ clusters coordinated by glutathione (21 mol% $[2Fe\text{-}2S]^{2+}$ and 79 mol% Fe^{2+}). (D) Mössbauer spectrum of a sample containing $[1Fe\text{-}0S]^{2+}$, $[2Fe\text{-}2S]^{2+}$, and $[4Fe\text{-}4\ S]^{2+}$ clusters coordinated by glutathione (10 mol% $[4Fe\text{-}4S]^{2+}$, 64 mol% $[2Fe\text{-}2S]^{2+}$, and 26 mol% Fe^{2+}). Panels B, C, and D are adapted from *Nature Chemistry*, Vol. 9, pp. 1229–1234, 2017, Springer Nature.[30] [Colour online.]

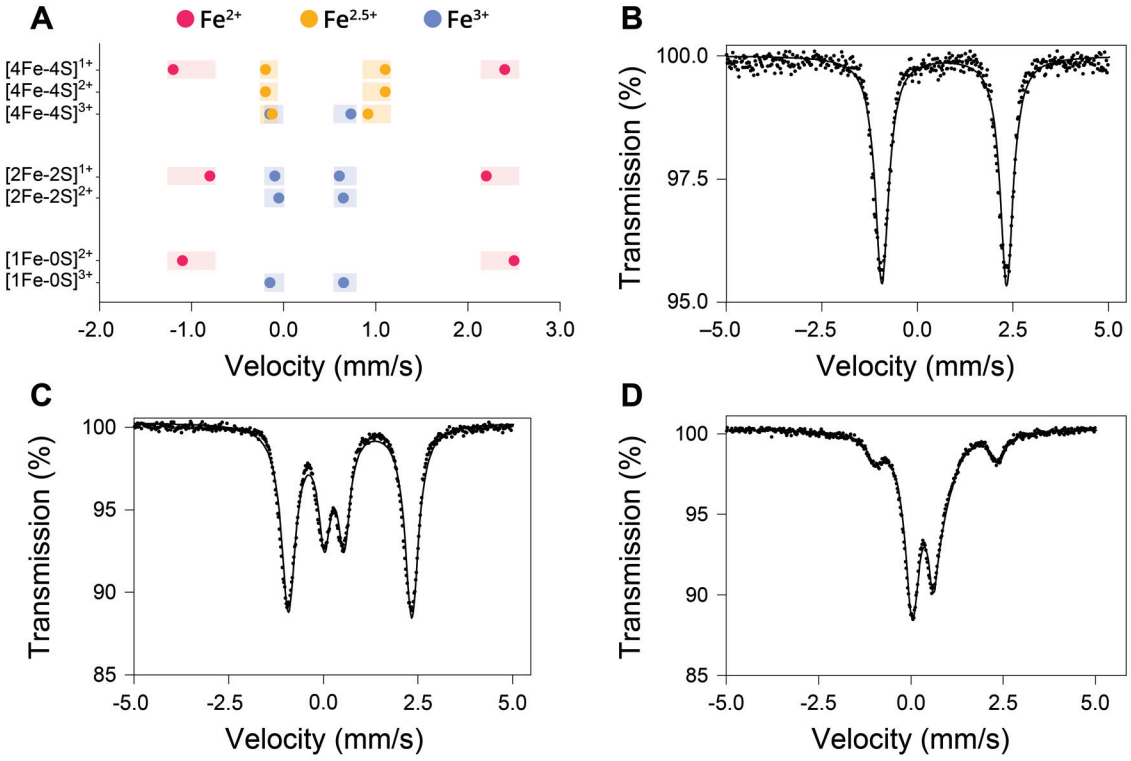

Differently than $[2Fe\text{-}2S]^{+}$ clusters, $[4Fe\text{-}4S]^{1+}$ clusters show faster relaxation and are only generally observable below 30 K.[23]

Mixtures of iron–sulfur clusters can be deconvoluted by exploiting the different relaxation times of each species. By using specific pulse sequences, the signal of a specific overlapped species might be selectively suppressed (REFINE Spectroscopy). Similarly, the effect of temperature on the signals of CW spectra can help determine the contributions of each iron–sulfur cluster in solution. For example, overlapped peaks of $[4Fe\text{-}4S]^{+}$ and $[2Fe\text{-}2S]^{+}$ clusters may be disentangled by experiments that reveal the progressive loss in intensity of one component, i.e., that of the $[4Fe\text{-}4S]^{+}$ cluster, with increasing temperature until ultimately leaving spectra solely consisting of the $[2Fe\text{-}2S]^{+}$ component, which remains unaffected by temperature until approximately 70 K.[23,126]

Mössbauer spectroscopy

Mössbauer spectroscopy is extremely useful in characterizing iron–sulfur clusters. This technique can identify every type of iron–sulfur cluster and every iron centre present within the sample in a way that reveals their spin state, oxidation state, and electronic structure and gives insight into the coordination sphere (Fig. 3).[127] Importantly, absorption is directly correlated to concentration, so the relative ratios of resonant nuclei can be discerned. Limitations of the technique include the need for ^{57}Fe labelled samples to absorb the γ-rays emitted from the ^{57}Co source,[128–130] and the need to either work with frozen samples at low temperatures or with precipitated complexes at higher temperature, i.e., the sample must be in the solid state to exploit the Mössbauer effect. If not in the solid state, nuclear recoil experienced by the emitting ^{57}Co and absorbing ^{57}Fe nuclei leads to energy loss and decreased absorption. If both emitting and absorbing nuclei are embedded in a solid matrix, the loss in nuclear recoil is minimized, allowing for resonance absorption of γ rays to occur. Spectra are obtained by scanning an energy range through the Doppler effect. That is, the source is physically moved at defined velocity to modulate the radiant energy, which is why the x axis of Mössbauer spectra is frequently expressed in millimetres per second. The y axis simply reports the transmission of γ rays.

Similar to EPR and paramagnetic NMR spectroscopies, the richness of the data obtained from Mössbauer spectroscopy is due in large part to hyperfine interactions, i.e., interactions between the nucleus and nearby electrons. Of these hyperfine interactions, the isomer shift (δ) provides a measure of the s electron density at the ^{57}Fe nucleus and is influenced by the p and d electrons by means of electrostatic shielding. δ is a key parameter for the assignment of iron oxidation states, due to the dependence of the charge density at the iron nucleus. Quadrupole splitting (ΔE_Q) typically reflects the population of the iron d orbitals, as well as the (a)symmetry of the ligand charges surrounding the ^{57}Fe nucleus.[131] In short, the electronic environment of the iron nucleus causes variations in the charge density that is detectable by Mössbauer spectroscopy (Fig. 3A). Similar to EPR spectroscopy, Mössbauer spectra require fitting to accurately decipher the spectral parameters associated with each species in the sample.

Usually, [1Fe-0S] gives rise to a single signal split into two peaks. Mössbauer spectra of oxidized rubredoxin ($[1Fe\text{-}0S]^{3+}$) is characterized by $\delta \sim 0.25$ mm/s and $\Delta E_Q \sim 0.5$–0.8 mm/s, whereas reduced rubredoxin ($[1Fe\text{-}0S]^{2+}$) is characterized by $\delta \sim 0.7$ mm/s and ΔE_Q 3.1–3.6 mm/s.[131–135] $[1Fe\text{-}0S]^{2+/3+}$ coordinated to cysteinyl peptides and other organic thiols show δ and ΔE_Q similar to that observed for rubredoxin (Fig. 3B).[28,114,132] [2Fe-2S] and [4Fe-4S] clusters give rise to more complex Mössbauer spectral patterns, especially when the iron ions do not share the same oxidation

state. $[2Fe\text{-}2S]^{2+}$ ferredoxins (S = 5/2) typically show a doublet for the two ferric ions that are antiferromagnetically coupled with $\delta \sim 0.3$ mm/s and $\Delta E_Q \sim 0.6$ mm/s, typical for complexes containing high-spin Fe^{3+} (Fig. 3C).[136–139] Mössbauer spectra of $[2Fe\text{-}2S]^{+}$ ferredoxins (S = 1/2) appear as a superimposition of spectra typical for thiol-coordinated Fe^{3+} and Fe^{2+} complexes, with equivalent intensities and distinct parameters (Fe^{2+}: $\delta \sim 0.7$ mm/s, $\Delta E_Q \sim 3$ mm/s; Fe^{3+}: $\delta \sim 0.25$ mm/s, $\Delta E_Q \sim 0.7$ mm/s) revealing valence-localized Fe^{3+} and Fe^{2+} sites.[136,140] Mössbauer spectra of $[2Fe\text{-}2S]^{2+}$ glutathione are similar to that of $[2Fe\text{-}2S]^{2+}$ ferredoxin.[29,33,141,142] Mössbauer spectra have been also reported for oxidized Rieske proteins, with signals (Fe^{2+}: δ = 0.74 mm/s, ΔE_Q = 3.05 mm/s; Fe^{3+} δ = 0.31 mm/s, ΔE_Q = 0.63 mm/s) that are similar to ferredoxins.[143]

$[4Fe\text{-}4S]^{2+}$ clusters (S = 0) are the best characterized by Mössbauer spectroscopy. All the iron ions are essentially indistinguishable with similar isomer shifts ($\delta \sim 0.45$ mm/s) and quadrupole splitting ($\Delta E_Q \sim 1.0$–1.3 mm/s) parameters.[15,49] Similar parameters are found for glutathione stabilized $[4Fe\text{-}4S]^{2+}$ cluster (Fig. 3D).[29] $[4Fe\text{-}4S]^{+}$ clusters (S = 1/2) are fit as an overlap of a diferrous pair antiferromagnetically coupled with a pair of $Fe^{2.5+}$ centres. For these systems, the isomer shift for the Fe^{2+} pair is $\delta \sim 0.60$ mm/s ($\Delta E_Q \sim 3.1$–3.6 mm/s) and $\delta \sim 0.49$ mm/s ($\Delta E_Q \sim 1.0$ mm/s) for the $Fe^{2.5+}$ pair.[144–146] The $[4Fe\text{-}4S]^{3+}$ cluster (S = 1/2) of HiPIPs show spectra indicative of a pair of Fe^{3+} ($\delta \sim 0.29$ mm/s and $\Delta E_Q \sim 0.88$ mm/s) that is antiferromagnetically coupled to that of a pair of $Fe^{2.5+}$ ($\delta \sim 0.40$ mm/s and $\Delta E_Q \sim 1.0$ mm/s).[147,148]

Reduction potential

The reduction potential of iron ions are strongly affected by solvent accessibility, the charges of neighboring residues, and the ligating residues.[149] Therefore, reduction potentials can be correlated to some extent with the type of iron–sulfur cluster, but corroborating evidence is typically needed (Fig. 4) (Supplementary Table S8).[150] The reduction potential of $[1Fe\text{-}0\ S]^{3+/2+}$ proteins are typically between 0 and –340 mV (vs SHE).[44,151] Synthetic $[1Fe\text{-}0S]^{3+/2+}$ analogues coordinated by small peptides tend to have more negative reduction potentials compared with their protein counterparts.[49,92,151] Ferredoxin-like $[2Fe\text{-}2S]^{2+/+}$ clusters display a wider range of reduction potentials from –150 to –400 mV (vs SHE).[55,150] Coordination by histidines, e.g., Rieske clusters, confers a more positive potential (0 to 400 mV),[152] although measured potentials are highly dependent on pH.[153] Here again, non-proteinaceous $[2Fe\text{-}2\ S]^{2+/+}$ complexes have a more negative reduction potential.[54,92] For example, Ueno et al. reported a synthetic [2Fe-2S] cluster coordinated by a small peptide that contained a CX_2C sequence with a reduction potential of –1100 mV (vs SHE).[53] The reduction potential of $[4Fe\text{-}4S]^{2+/+}$ (i.e., low potential, ferredoxin-like) proteins fall in the range of –200 to –800 mV (vs SHE),[58,62] whereas $[4Fe\text{-}4S]^{3+/2+}$ (i.e., high potential, HiPIP-like) are typically between +100 and +500 mV (vs SHE).[68] Synthetic approaches are capable of producing low potential analogues in aqueous solution.[30,57,64,66,106,154] Analogues of HiPIPs have been more difficult to synthesize, with one successful example in tetrahydrofuran reported (–180 mV vs SHE).[155] Measurements of reduction potential can be combined with spectroscopic techniques to more deeply characterize the kinetics underlying redox activity. Such spectroelectrochemistry is generally applied to the study of iron–sulfur proteins by exploiting UV–vis.[156] Recently, this approach was used to characterize iron–sulfur oligopeptides.[151] However, as with several techniques, measurements can be challenging when analyzing solutions of mixtures of iron–sulfur clusters.

Conclusions

Iron–sulfur clusters are ancient biological cofactors that have been investigated for over half a century.[152] Nevertheless, these metallocofactors can be challenging to characterize when coordinated to multiple, small oligopeptides (≤ hexapeptide), because the resulting solutions are typically in equilibrium between multiple types of iron–sulfur clusters each absorbing in the same region. Mössbauer spectroscopy is an excellent method to conclusively determine the type of clusters present, especially when coupled with EPR spectroscopy, but Mössbauer spectroscopy is not commonly available. Much can still be deciphered through more readily available instrumentation, such as UV–vis, CD, and NMR spectroscopies. The latter has been underexploited despite the wide availability of NMR spectrometers and the ease in acquiring such spectra. Resonance Raman is a good technique to characterize iron–sulfur clusters, but instrumentation and expertise are not always locally available. Electrochemistry not only gives insight into the potential activity of the metallopeptide, but can also be used to indicate the possible type of iron–sulfur cluster present through comparisons with previous reports. Of course, data from structural methodologies, such as X-ray crystallography, are superior to some of the described techniques. Such methods were not addressed here because of the difficulty in obtaining structures from solutions containing a mixture of species. Despite the difficulties, there is much to be gained from a deeper understanding of the assembly and coordination chemistry of iron–sulfur oligopeptides. Unearthing such ancient and central chemistry may very well reveal mechanisms at the heart of biological energetics.

Fig. 4. Representation of published reduction potentials of [1Fe-0S] (yellow), [2Fe-2S] (red), and [4Fe-4S] (blue) clusters. Peptides are represented as circles. Proteins are indicated as squares, except for *Chromatium vinosum* HiPIP, which is shown as a diamond. [Colour online.]

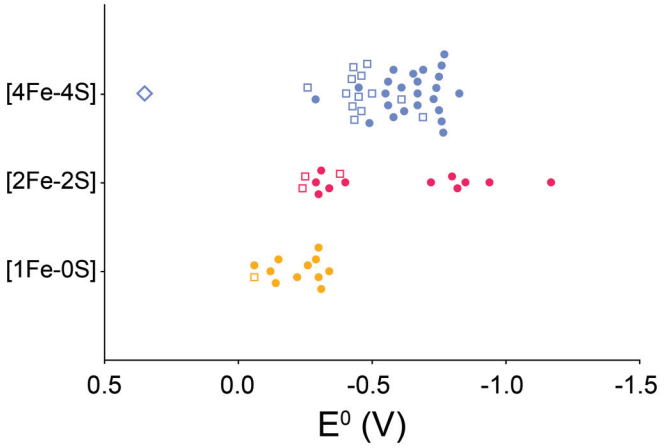

Supplementary data

Supplementary data are available with the article at https://doi.org/10.1139/cjc-2021-0237.

Acknowledgements

This project received funding from the European Union's Horizon 2020 research and innovation programme under the Marie Skłodowska–Curie grant agreement No 813873. We also thank the Simons Foundation (290358FY18 and 290358FY19) and the Natural Sciences and Engineering Research Council of Canada (NSERC) [RGPIN-2020-04375] for funding.

References

(1) Williams, R. J. P. *The chemistry of evolution*; Elsevier. 2006; pp. 1–34.
(2) Casareno, R.; Li, D.; Cowan, J. A. *J. Am. Chem. Soc.* **1995**, *117* (44), 11011. doi:10.1021/ja00149a026.
(3) Imlay, J. A. *Mol. Microbiol.* **2006**, *59* (4), 1073. doi:10.1111/j.1365-2958.2006.05028.x.

(4) Daniel, R. M.; Danson, M. J. *J. Mol. Evol*. **1995**, *40* (6), 559. doi:10.1007/BF00160501.
(5) Belmonte, L.; Mansy, S. S. *Elements*, **2016**, *12* (6), 413. doi:10.2113/gselements.12.6.413.
(6) Calvin, M. *Science*, **1959**, *130* (3383), 1170. doi:10.1126/science.130.3383.1170.
(7) Muchowska, K. B.; Varma, S. J.; Moran, J. *Nature*, **2019**, *569* (7754), 104. doi:10.1038/s41586-019-1151-1.
(8) Keller, M. A.; Turchyn, A. V.; Ralser, M. *Mol. Syst. Biol*. **2014**, *10* (725), 725. doi:10.1002/msb.20145228.
(9) Coggins, A. J.; Powner, M. W. *Nat. Chem*. **2017**, *9* (4), 310. doi:10.1038/nchem.2624.
(10) Green, N. J.; Xu, J.; Sutherland, J. D. *J. Am. Chem. Soc*. **2021**, *143* (19), 7219. doi:10.1021/jacs.1c01839.
(11) Stubbs, R. T.; Yadav, M.; Krishnamurthy, R.; Springsteen, G. *Nat. Chem*. **2020**, *12* (11), 1016. doi:10.1038/s41557-020-00560-7.
(12) Okafor, C. D.; Lanier, K. A.; Petrov, A. S.; Athavale, S. S.; Bowman, J. C.; Hud, N. V.; Williams, L. D. *Nucleic Acids Res*. **2017**, *45* (7), 3634. doi:10.1093/nar/gkx171.
(13) Nakamura, T.; Naguro, I.; Ichijo, H. *Biochim. Biophys. Acta Gen. Subj*. **2019**, *1863* (9), 1398. doi:10.1016/j.bbagen.2019.06.010.
(14) Mailloux, R. J.; McBride, S. L.; Harper, M.-E. *Trends Biochem. Sci*. **2013**, *38* (12), 592. doi:10.1016/j.tibs.2013.09.001.
(15) Wu, G.; Fang, Y.-Z.; Yang, S.; Lupton, J. R.; Turner, N. D. *J. Nutr*. **2004**, *134* (3), 489. doi:10.1093/jn/134.3.489.
(16) Meister, A. *J. Biol. Chem*. **1988**, *263* (33), 17205. doi:10.1016/S0021-9258(19)77815-6.
(17) Johnson, D. C.; Dean, D. R.; Smith, A. D.; Johnson, M. K. *Annu. Rev. Biochem*. **2005**, *74* (1), 247. doi:10.1146/annurev.biochem.74.082803.133518.
(18) Link, T. A. *Adv. Inorg. Chem*. **1999**, *47*, 83. doi:10.1016/S0898-8838(08)60077-X.
(19) Meyer, J. *J. Biol. Inorg. Chem*. **2008**, *13* (2), 157. doi:10.1007/s00775-007-0318-7.
(20) Yoo, S. J.; Meyer, J.; Münck, E. *J. Am. Chem. Soc*. **1999**, *121*, (44), 10450. doi:10.1021/ja992829n.
(21) Yao, W.; Gurubasavaraj, P. M.; Holland, P. L. *Struct. Bond*. **2014**, 160. doi:10.1007/430_2012_81.
(22) Sweeney, W.; Rabinowitz, J.; Yoch, D. *J. Biol. Chem*. **1975**, *250* (19), 7842. doi:10.1016/S0021-9258(19)40892-2.
(23) Angove, H. C.; Yoo, S. J.; Burgess, B. K.; Münck, E. *J. Am. Chem. Soc*. **1997**, *119* (37), 8730. doi:10.1021/ja9712837.
(24) Beinert, H.; Holm, R. H.; MüNck, E. *Science*, **1997**, *277* (5326), 653. doi:10.1126/science.277.5326.653.
(25) Johnson, M. K.; Smith, A. D. *Encyclopedia of inorganic and bioinorganic chemistry*; John Wiley & Sons, Ltd., Chichester, UK. 2011.
(26) Venkateswara Rao, P.; Holm, R. H. *Chem. Rev*. **2004**, *104* (2), 527. doi:10.1021/cr020615+.
(27) Beinert, H. *J. Biol. Inorg. Chem*. **2000**, *5* (1), 2. doi:10.1007/s007750050002.
(28) Varma, S. J.; Muchowska, K. B.; Chatelain, P.; Moran, J. *Nat. Ecol. Evol*. **2018**, *2* (6), 1019. doi:10.1038/s41559-018-0542-2.
(29) Scintilla, S.; Bonfio, C.; Belmonte, L.; Forlin, M.; Rossetto, D.; Li, J.; et al. *Chem. Commun*. **2016**, *52* (92), 13456. doi:10.1039/C6CC07912A.
(30) Bonfio, C.; Valer, L.; Scintilla, S.; Shah, S.; Evans, D. J.; Jin, L.; et al. *Nat. Chem*. **2017**, *9* (12), 1229. doi:10.1038/nchem.2817.
(31) Kim, J. D.; Pike, D. H.; Tyryshkin, A. M.; Swapna, G. V. T.; Raanan, H.; Montelione, G. T.; Nanda, V.; Falkowski, P. G. *J. Am. Chem. Soc*. **2018**, *140* (36), 11210. doi:10.1021/jacs.8b07553.
(32) Sanden, S. A.; Yi, R.; Hara, M.; McGlynn, S. E. *Chem. Commun*. **2020**, *56* (80), 11989. doi:10.1039/D0CC04078A.
(33) Holm, R. H. *Acc. Chem. Res*. **1977**, *10* (12), 427. doi:10.1021/ar50120a001.
(34) Qi, W.; Li, J.; Chain, C. Y.; Pasquevich, G. A.; Pasquevich, A. F.; Cowan, J. A. *J. Am. Chem. Soc*. **2012**, *134* (26), 10745. doi:10.1021/ja302186j.
(35) Eck, R. V.; Dayhoff, M. O. *Science*, **1966**, *152* (3720), 363. doi:10.1126/science.152.3720.363.
(36) Alva, V.; Söding, J.; Lupas, A. N. *Elife*, **2015**, *4*, e09410. doi:10.7554/eLife.09410.
(37) Mulholland, S. E.; Gibney, B. R.; Rabanal, F.; Dutton, P. L. *J. Am. Chem. Soc*. **1998**, *120* (40), 10296. doi:10.1021/ja981279a.
(38) Belmonte, L.; Mansy, S. S. *J. Chem. Inf. Model*. **2017**, *57* (12), 3162. doi:10.1021/acs.jcim.7b00468.
(39) Galambas, A.; Miller, J.; Jones, M.; McDaniel, E.; Lukes, M.; Watts, H.; et al. *J. Biol. Inorg. Chem*. **2019**, *24* (6), 793. doi:10.1007/s00775-019-01708-8.
(40) Betinol, I. O.; Nader, S.; Mansy, S. S. *Anal. Biochem*. **2021**, *629*, 114269. doi:10.1016/j.ab.2021.114269.
(41) Mao, Z.; Liou, S.-H.; Khadka, N.; Jenney, F. E.; Goodin, D. B.; Seefeldt, L. C.; et al. *Biochemistry*, **2018**, *57*, (6), 978. doi:10.1021/acs.biochem.7b01159.
(42) Moura, I.; Bruschi, M.; Le Gall, J.; Moura, J. J. G.; Xavier, A. V. *Biochem. Biophys. Res. Commun*. **1977**, *75* (4), 1037. doi:10.1016/0006-291X(77)91486-3.
(43) Maelia, L. E.; Millar, M.; Koch, S. A. *Inorg. Chem*. **1992**, *31* (22), 4594. doi:10.1021/ic00048a029.
(44) Sugiura, Y.; Ishizu, K.; Kimura, T. *Biochem. Biophys. Res. Commun*. **1974**, *60* (1), 334. doi:10.1016/0006-291X(74)90209-5.
(45) Hamed, M. Y.; Silver, J.; Wilsonx, M. T. *Inorg. Chim. Acta*, **1983**, *78* (C), 1. doi:10.1016/S0020-1693(00)86480-4.
(46) Nakata, M.; Ueyama, N.; Fuji, M.; Nakamura, A.; Wada, K.; Matsubara, H. *Biochim. Biophys. Acta Protein Struct. Mol. Enzymol*. **1984**, *788* (3), 306. doi:10.1016/0167-4838(84)90042-6.
(47) Ueyama, N.; Nakata, M.; Fuji, M. A.; Terakawa, T.; Nakamura, A. *Inorg. Chem*. **1985**, *24* (14), 2190. doi:10.1021/ic00208a016.
(48) Sun, W. Y.; Ueyama, N.; Nakamura, A. *Inorg. Chem*. **1991**, *30* (21), 4026. doi:10.1021/ic00021a011.
(49) Nivorozhkin, A. L.; Segal, B. M.; Musgrave, K. B.; Kates, S. A.; Hedman, B.; Hodgson, K. O.; Holm, R. H. *Inorg. Chem*. **2000**, *39* (11), 2306. doi:10.1021/ic990421l.
(50) Kubas, A. *Theor. Chem. Acc*. **2020**, *139*, 120. doi:10.1007/s00214-020-02635-7.
(51) Balasubramaniam, A.; Cocouvanis, D. *Inorganica Chim. Acta*, **1983**, *78*, L35. doi:10.1016/S0020-1693(00)86469-5.
(52) Ueyama, N.; Ueno, S.; Nakata, M.; Nakamura, A. *Bull. Chem. Soc. Jpn*. **1984**, *57* (4), 984. doi:10.1246/bcsj.57.984.
(53) Ueno, S.; Ueyama, N.; Nakamura, A.; Tukihara, T. *Inorg. Chem*. **1986**, *25* (7), 1000. doi:10.1021/ic00227a023.
(54) Ueyama, N.; Ueno, S.; Nakamura, A.; Wada, K.; Matsubara, H.; Kumagai, S.-I.; Sakakibara, S.; Tsukihara, T. *Biopolymers*, **1992**, *32* (11), 1535. doi:10.1002/bip.360321111.
(55) Xia, B.; Cheng, H.; Bandarian, V.; Reed, G. H.; Markley, J.L. *Biochemistry*, **1996**, *35* (29), 9488. doi:10.1021/bi960467f.
(56) Konkle, M. E.; Muellner, S. K.; Schwander, A. L.; Dicus, M. M.; Pokhrel, R.; Britt, R. D.; Taylor, A. B.; Hunsicker-Wang, L. M. *Biochemistry*, **2009**, *48* (41), 9848. doi:10.1021/bi901126u.
(57) Hill, C. L.; Renaud, J.; Holm, R. H.; Mortenson, L. E. *J. Am. Chem. Soc*. **1977**, *99* (8), 2549. doi:10.1021/ja00450a024.
(58) Emptage, M. H.; Kent, T. A.; Kennedy, M. C.; Beinert, H.; Münck, E. *Proc. Natl. Acad. Sci. U. S. A*. **1983**, *80* (15), 4674. doi:10.1073/pnas.80.15.4674.
(59) Phillips, J. D.; Guo, B.; Yu, Y.; Brown, F. M.; Leibold, E. A. *Biochemistry*, **1996**, *35* (49), 15704. doi:10.1021/bi960653l.
(60) Buchanan, B. B.; Lovenberg, W.; Rabinowitz, J. C. *Proc. Natl. Acad. Sci. U. S. A*. **1963**, *49*, 345. doi:10.1073/pnas.49.3.345.
(61) Yang, S. S.; Ljungdahl, L. G.; LeGall, J. *J. Bacteriol*. **1977**, *130* (3), 1084. doi:10.1128/jb.130.3.1084-1090.1977.
(62) Stombaugh, N. A.; Sundquist, J. E.; Burris, R. H.; Orme-Johnson, W. H. *Biochemistry*, **1976**, *15* (12), 2633. doi:10.1021/bi00657a024.
(63) Devanathan, T.; Akagi, J. M.; Hersh, R. T.; Himes, R. H. *J. Biol. Chem*. **1969**, *244* (11), 2846. doi:10.1016/S0021-9258(18)91704-7.
(64) DePamphilis, B. V.; Averill, B. A.; Herskovitz, T.; Que, L.; Holm, R. H. *J. Am. Chem. Soc*. **1974**, *96* (13), 4159. doi:10.1021/ja00820a017.
(65) Ueyama, N.; Kajiwara, A.; Terakawa, T.; Ueno, S.; Nakamura, A. *Inorg. Chem*. **1985**, *24* (26), 4700. doi:10.1021/ic00220a053.
(66) Ueyama, N.; Terakawa, T.; Nakata, M.; Nakamura, A. *J. Am. Chem. Soc*. **1983**, *105* (24), 7098. doi:10.1021/ja00362a013.
(67) Kennedy, M. C.; Kent, T. A.; Emptage, M.; Merkle, H.; Beinert, H.; Münck, E. *J. Biol. Chem*. **1984**, *259* (23), 14463. doi:10.1016/S0021-9258(17)42622-6.
(68) Moulis, J. M.; Lutz, M.; Gaillard, J.; Noodleman, L. *Biochemistry*, **1988**, *27*, 8712. doi:10.1021/bi00424a004.
(69) Elliott, J. I.; Ljungdahl, L. G. *J. Bacteriol*. **1982**, *151* (1), 328. doi:10.1128/jb.151.1.328-333.1982.
(70) Bych, K.; Kerscher, S.; Netz, D. J. A.; Pierik, A. J.; Zwicker, K.; Huynen, M. A.; et al. *EMBO J*. **2008**, *27* (12), 1736. doi:10.1038/emboj.2008.98.
(71) Hochkoeppler, A.; Kofod, P.; Ferro, G.; Ciurli, S. *Arch. Biochem. Biophys*. **1995**, *322*, 313. doi:10.1006/abbi.1995.1469.
(72) Nader, S.; Betinol, I. O.; Mansy, S. S. Fit-FeS: spectral decomposition of iron–sulfur clusters. Reference spectra included 2021.
(73) Stephens, P. J.; Dunn, J. B. R.; Rao, K. K.; Hall, D. O.; Thomson, A. J.; Keiderling, T. A.; Rawlings, J. *Biochemistry*, **1978**, *17* (22), 4770. doi:10.1021/bi00615a026.
(74) Kreuger, J.; Salmivirta, M.; Sturiale, L.; Giménez-Gallego, G.; Lindahl, U. *J. Biol. Chem*. **2001**, *276* (33), 30744. doi:10.1074/jbc.M102628200.
(75) Dos Santos, P. C. *Methods in molecular biology*; Dos Santos, P. C., Editor; Springer US, New York, NY. 2021; Vol. 2353.
(76) Webert, H.; Freibert, S. A.; Gallo, A.; Heidenreich, T.; Linne, U.; Amlacher, S.; et al. *Nat. Commun*. **2014**, *5*, 5013. doi:10.1038/ncomms6013.
(77) Wachnowsky, C.; Fidai, I.; Cowan, J. A. *FEBS Lett*. **2016**, *590* (24), 4531. doi:10.1002/1873-3468.12491.
(78) Freibert, S. A.; Weiler, B. D.; Bill, E.; Pierik, A. J.; Mühlenhoff, U.; Lill, R. *Methods Enzymol*. **2018**, *599*, 197. doi:10.1016/bs.mie.2017.11.034. PMID:29746240.
(79) Stephens, P. J.; Thomson, A. J.; Keiderling, T. A.; Rawlings, J.; Rao, K. K.; Hall, D. O. *Proc. Natl. Acad. Sci. U.S.A*. **1978**, *75* (11), 5273. doi:10.1073/pnas.75.11.5273.
(80) Spiro, T. G.; Czernuszewicz, R. S. *Methods Enzymol*. **1995**, *246* (1985), 416. doi:10.1016/0076-6879(95)46020-9. PMID:7752933.
(81) Todorovic, S.; Teixeira, M. *J. Biol. Inorg. Chem*. **2018**, *23* (4), 647. doi:10.1007/s00775-018-1533-0.
(82) Czernuszewicz, R. S.; Kilpatrick, L. T. K.; Koch, S. A.; Spiro, T. G. *J. Am. Chem. Soc*. **1994**, *116* (16), 7134. doi:10.1021/ja00095a017.
(83) Han, S.; Czernuszewicz, R. S.; Spiro, T. G. *J. Am. Chem. Soc*. **1989**, *111* (10), 3496. doi:10.1021/ja00192a002.
(84) Fu, W.; Drozdzewski, P. M.; Davies, M. D.; Sligar, S. G.; Johnson, M. K. *Proteins J. Biol. Chem*. **1992**, *267* (22), 15502. doi:10.1016/S0021-9258(19)49563-X.
(85) Iwasaki, T.; Kounosu, A.; Aoshima, M.; Ohmori, D.; Imai, T.; Urushiyama, A.; Cosper, N. J.; Scott, R. A. *J. Biol. Chem*. **2002**, *277*, 39642. doi:10.1074/jbc.M207312200.

(86) Kilpatrick, L. K.; Kennedy, M. C.; Beinert, H.; Czernuszewicz, R. S.; Spiro, T. G.; Qiu, D. *J. Am. Chem. Soc.* **1994**, *116* (9), 4053. doi:10.1021/ja00088a046.
(87) Kowalsky, A. *Biochemistry*, **1965**, *4* (11), 2382. doi:10.1021/bi00887a018.
(88) Bertini, I.; Luchinat, C.; Rosato, A. *Adv. Inorg. Chem*. **1999**, *47*, 251. doi:10.1016/S0898-8838(08)60080-X.
(89) Banci, L.; Camponeschi, F.; Ciofi-Baffoni, S.; Piccioli, M. *J. Biol. Inorg. Chem*. **2018**, *23* (4), 665. doi:10.1007/s00775-018-1552-x.
(90) Bertini, I.; Luchinat, C.; Parigi, G.; Pierattelli, R. *ChemBioChem*, **2005**, *6* (9), 1536. doi:10.1002/cbic.200500124.
(91) Bertini, I.; Luchinat, C. *NMR of paramagnetic molecules in biological systems*; Benjamin-Cummings Publishing Company. 1986.
(92) Nakamura, A.; Ueyama, N. *Adv. Inorg. Chem*. **1989**, *33*, 39. doi:10.1016/S0898-8838(08)60193-2.
(93) Werth, M. T.; Kurtz, D. M.; Moura, I.; LeGall, J. *J. Am. Chem. Soc*. **1987**, *109*, 273. doi:10.1021/ja00235a042.
(94) Ueyama, N.; Sun, W. Y.; Nakamura, A. *Inorg. Chem*. **1992**, *31* (20), 4053. doi:10.1021/ic00046a013.
(95) Xia, B.; Pikus, P. D.; Xia, W.; McClay, K.; Steffan, R. J.; Chae, Y. K.; et al. *Biochemistry*, **1999**, *38* (2), 727. doi:10.1021/bi981851a.
(96) Salmeen, I.; Palmer, G. *Arch. Biochem. Biophys*. **1972**, *150* (2), 767. doi:10.1016/0003-9861(72)90096-3.
(97) Skjeldal, L.; Markley, J.L .; Coghlan, V. M.; Vickery, L. E. *Biochemistry*, **1991**, *30* (37), 9078. doi:10.1021/bi00101a024.
(98) Chan, T. M.; Markley, J. L. *Biochemistry*, **1983**, *22* (25), 6008. doi:10.1021/bi00294a048.
(99) Xia, B.; Jenk, D.; LeMaster, D. M.; Westler, W. M.; Markley, J. L. *Arch. Biochem. Biophys*. **2000**, *373* (2), 328. doi:10.1006/abbi.1999.1576.
(100) Dugad, L. B.; La Mar, G. N.; Banci, L.; Bertini, I. *Biochemistry*, **1990**, *29* (9), 2263. doi:10.1021/bi00461a009.
(101) Nagayama, K.; Ozaki, Y.; Kyogoku, Y.; Hase, T.; Matsubara, H. *J. Biochem*. **1983**, *94* (3), 893. doi:10.1093/oxfordjournals.jbchem.a134432.
(102) Antonkine, M. L.; Bentrop, D.; Bertini, I.; Luchinat, C.; Shen, G.; Bryant, D. A.; Stehlik, D.; Golbeck, J. H. *J. Biol. Inorg. Chem*. **2000**, *5* (3), 381. doi:10.1007/PL00010667.
(103) Bertini, I.; Briganti, F.; Luchinat, C.; Scozzafava, A. *Inorg. Chem*. **1990**, *29* (10), 1874. doi:10.1021/ic00335a023.
(104) Lanzilotta, W. N.; Holz, R. C.; Seefeldt, L. C. *Biochemistry*, **1995**, *34* (48), 15646. doi:10.1021/bi00048a007.
(105) Lebrun, E.; Simenel, C.; Guerlesquin, F.; Delepierre, M. *Magn. Reson. Chem*. **1996**, *34* (11), 873. doi:10.1002/(SICI)1097-458X(199611)34:11<873::AID-OMR983>3.0.CO;2-D.
(106) Bertini, I.; Capozzi, F.; Ciurli, S.; Luchinat, C.; Messori, L.; Piccioli, M. *J. Am. Chem. Soc*. **1992**, *114* (9), 3332. doi:10.1021/ja00035a026.
(107) Nieman, J.; Naaktgeboren, A. J.; Reedijk, J. *Inorg. Chim. Acta*, **1984**, *93* (1), L9. doi:10.1016/S0020-1693(00)85947-2.
(108) Que, L.; Anglin, J. R.; Bobrik, M. A.; Davison, A.; Holm, R. H. *J. Am. Chem. Soc*. **1974**, *96* (19), 6042. doi:10.1021/ja00826a014.
(109) Hagen, K. S.; Watson, A. D.; Holm, R. H. *J. Am. Chem. Soc*. **1983**, *105*, 3905. doi:10.1021/ja00350a028.
(110) Roessler, M. M.; Salvadori, E. *Chem. Soc. Rev*. **2018**, *47* (8), 2534. doi:10.1039/C6CS00565A.
(111) Roessler, M. M.; King, M. S.; Robinson, A. J.; Armstrong, F. A.; Harmer, J.; Hirst, J. *Proc. Natl. Acad. Sci. U.S.A*. **2010**, *107* (5), 1930. doi:10.1073/pnas.0908050107.
(112) Peisach, J.; Blumberg, W. E.; Lode, E. T.; Coon, M. J. *J. Biol. Chem*. **1971**, *246* (19), 5877. doi:10.1016/S0021-9258(18)61807-1.
(113) Yoon, K.-S.; Hille, R.; Hemann, C.; Tabita, F. R. *J. Biol. Chem*. **1999**, *274* (42), 29772. doi:10.1074/jbc.274.42.29772.
(114) Lee, W. Y.; Brune, D. C.; Lobrutto, R.; Blankenship, R. E. *Arch. Biochem. Biophys*. **1995**, *318* (1), 80. doi:10.1006/abbi.1995.1207.
(115) Yang, S.-S.; Ljungdahl, L. G.; Dervartanian, D. V.; Watt, G. D. *Biochim. Biophys. Acta*, **1980**, *590*, 24. doi:10.1016/0005-2728(80)90143-7.
(116) LeGall, J.; Liu, M. Y.; Gomes, C. M.; Braga, V.; Pacheco, I.; Regalla, M.; Xavier, A. V.; Teixeira, M. *FEBS Lett*. **1998**, *429* (3), 295. doi:10.1016/S0014-5793(98)00610-3.
(117) Werth, M. T.; Kurtz, D. M.; Howes, B. D.; Boi, H. H. *Inorg. Chem*. **1989**, *28* (7), 1357. doi:10.1021/ic00306a028.
(118) Knapp, M. J.; Krzystek, J.; Brunel, L.-C.; Hendrickson, D.N. *Inorg. Chem*. **2000**, *39* (2), 281. doi:10.1021/ic9910054.
(119) Coghlan, V. M.; Vickery, L. E. *Proc. Natl. Acad. Sci. U.S.A*. **1989**, *86* (3), 835. doi:10.1073/pnas.86.3.835.
(120) Boxhammer, S.; Glaser, S.; Kühl, A.; Wagner, A. K.; Schmidt, C.L. *BioMetals*, **2008**, *21* (4), 459. doi:10.1007/s10534-008-9134-y.
(121) Mascharak, P. K.; Papaefthymiou, G.C .; Frankel, R. B.; Holm, R. H. *J. Am. Chem. Soc*. **1981**, *103* (20), 6110. doi:10.1021/ja00410a021.
(122) Zanello, P. *Coord. Chem. Rev*. **2017**, *335*, 172. doi:10.1016/j.ccr.2016.10.003.
(123) Sweeney, W. V.; Rabinowitz, J. C. *Annu. Rev. Biochem*. **1980**, *49* (1), 139. doi:10.1146/annurev.bi.49.070180.001035.
(124) Berto, P.; Di Valentin, M.; Cendron, L.; Vallese, F.; Albertini, M.; Salvadori, E.; et al. *Biochim. Biophys. Acta Bioenerg*. **2012**, *1817* (12), 2149. doi:10.1016/j.bbabio.2012.09.004.
(125) Cammack, R.; MacMillan, F. Electron magnetic resonance of iron–sulfur proteins in electron-transfer chains: resolving complexity; In: *Metals in Biology*; Biological Magnetic Resonance; Springer, New York, NY. 2009; pp. 11–44.
(126) Garcia-Serres, R.; Clémancey, M.; Latour, J.-M.; Blondin, G. *J. Biol. Inorg. Chem*. **2018**, *23* (4), 635. doi:10.1007/s00775-018-1534-z.
(127) Yoo, S. J.; Angove, H. C.; Papaefthymiou, V.; Burgess, B. K.; Münck, E. *J. Am. Chem. Soc*. **2000**, *122* (20), 4926. doi:10.1021/ja000254k.
(128) Charitou, G.; Tsertos, C.; Parpottas, Y.; Kleanthous, M.; Lederer, C. W.; Phylactides, M. *Eur. Biophys. J*. **2019**, *48* (7), 635. doi:10.1007/s00249-019-01389-w.
(129) Clémancey, M.; Blondin, B.; Latour, J.-M.; Garcia-Serres, R. Mössbauer spectroscopy. In: *Metalloproteins*; Fontecilla-Camps, J. C.; Nicolet, Y., Editors. Methods in Molecular Biology (Methods and Protocols), Vol. 1122. Humana Press, Totowa, NJ; Vol. 1122. 2014; pp. 153–170.
(130) Gütlich, P.; Bill, E.; Trautwein, A. X. *Mössbauer spectroscopy and transition metal chemistry*; Vol. 50. Springer Berlin Heidelberg, Berlin, Heidelberg; 2011.
(131) Vrajmasu, V. V.; Bominaar, E. L.; Meyer, J.; Münck, E. *Inorg. Chem*. **2002**, *41* (24), 6358. doi:10.1021/ic020508y.
(132) Rao, K. K.; Evans, M. C. W.; Cammack, R.; Hall, D. O.; Thompson, C. L.; Jackson, P. J.; Johnson, C. E. *Biochem. J*. **1972**, *129*, 1063. doi:10.1042/bj1291063.
(133) Phillips, W. D.; Poe, M.; Weiher, J. F.; McDonald, C. C.; Lovenberg, W. *Nature*, **1970**, *227* (5258), 574. doi:10.1038/227574a0.
(134) LeGall, J.; Prickril, B. C.; Moura, I.; Xavier, A. V.; Moura, J. J. G.; Huynh Boi, H. *Biochemistry*, **1988**, *27* (5), 1636. doi:10.1021/bi00405a037.
(135) Anderson, R. E.; Dunham, W. R.; Sands, R. H.; Bearden, A. J.; Crespi, H. L. *Biochim. Biophys. Acta Bioenerg*. **1975**, *408* (3), 306. doi:10.1016/0005-2728(75)90132-2.
(136) Muenck, E.; Debrunner, P. G.; Tsibris, J. C. M.; Gunsalus, I.C. *Biochemistry*, **1972**, *11* (5), 855. doi:10.1021/bi00755a027.
(137) Meyer, J.; Clay, M. D.; Johnson, M. K.; Stubna, A.; Münck, E.; Higgins, C.; Wittung-Stafshede, P. *Biochemistry*, **2002**, *41* (9), 3096. doi:10.1021/bi015981m.
(138) Dunham, W. R.; Bearden, A. J.; Salmeen, I. T.; Palmer, G.; Sands, R. H.; Orme-Johnson, W. H.; Beinert, H. *Biochim. Biophys. Acta Bioenerg*. **1971**, *253* (1), 134. doi:10.1016/0005-2728(71)90240-4.
(139) Wu, C.; Jiang, W.; Krebs, C.; Stubbe, J. *Biochemistry*, **2007**, *46* (41), 11577. doi:10.1021/bi7012454.
(140) Pandelia, M. E.; Lanz, N. D.; Booker, S. J.; Krebs, C. *Biochim. Biophys. Acta Mol. Cell Res*. **2015**, *1853* (6), 1395. doi:10.1016/j.bbamcr.2014.12.005.
(141) Ballmann, J.; Albers, A.; Demeshko, S.; Dechert, S.; Bill, E.; Bothe, E.; Ryde, U.; Meyer, F. *Angew. Chem. Int. Ed*. **2008**, *47* (49), 9537. doi:10.1002/anie.200803418.
(142) Fee, J. A.; Findling, K. L.; Yoshida, T.; Hille, R.; Tarr, G. E.; Hearshen, D. O.; et al. *J. Biol. Chem*. **1984**, *259* (1), 124. doi:10.1016/S0021-9258(17)43630-1.
(143) Chandramouli, K.; Unciuleac, M.-C.; Naik, S.; Dean, D. R.; Huynh, B. H.; Johnson, M. K. *Biochemistry*, **2007**, *46* (23), 6804. doi:10.1021/bi6026659.
(144) Khoroshilova, N.; Popescu, C.; Munck, E.; Beinert, H.; Kiley, P. J. *Proc. Natl. Acad. Sci. U.S.A*. **1997**, *94* (12), 6087. doi:10.1073/pnas.94.12.6087.
(145) Middleton, P.; Dickson, D. P. E.; Johnson, C. E.; Rush, J. D. *Eur. J. Biochem*. **1978**, *88* (1), 135. doi:10.1111/j.1432-1033.1978.tb12430.x.
(146) Bertini, I.; Campos, A. P.; Teixeira, M.; Luchinat, C. *J. Inorg. Biochem*. **1993**, *52* (3), 227. doi:10.1016/0162-0134(93)80043-9.
(147) Kyritsis, P.; Kümmerle, R.; Huber, J. G.; Gaillard, J.; Guigliarelli, B.; Popescu, C.; Münck, E.; Moulis, J.-M. *Biochemistry*, **1999**, *38* (19), 6335. doi:10.1021/bi982894u.
(148) Liu, J.; Chakraborty, S.; Hosseinzadeh, P.; Yu, Y.; Tian, S.; Petrik, I.; Bhagi, A.; Lu, Y. *Chem. Rev*. **2014**, *114* (8), 4366. doi:10.1021/cr400479b. PMID:24758379.
(149) Bonfio, C. *Dalton Trans*. **2021**, *50* (3), 801. doi:10.1039/D0DT03947K.
(150) Bak, D. W.; Elliott, S. J. *Curr. Opin. Chem. Biol*. **2014**, *19* (1), 50. doi:10.1016/j.cbpa.2013.12.015.
(151) Bonfio, C.; Godino, E.; Corsini, M.; Fabrizi de Biani, F.; Guella, G.; Mansy, S. S. *Nat. Catal*. **2018**, *1*, 616. doi:10.1038/s41929-018-0116-3.
(152) Link, T. A.; Hagen, W. R.; Pierik, A. J.; Assmann, C.; von Jagonw, G. *Eur. J. Biochem*. **1992**, *208*, 685. (doi:10.1111/j.1432-1033.1992.tb17235.x.
(153) Bellei, M.; Battistuzzi, G.; Wu, S.; Mansy, S. S.; Cowan, J. A.; Sola, M. *J. Inorg. Biochem*. **2010**, *104* (6), 691. doi:10.1016/j.jinorgbio.2010.03.001.
(154) Kennedy, M. L.; Gibney, B. R. *J. Am. Chem. Soc*. **2002**, *124* (24), 6826. doi:10.1021/ja0171613.
(155) Ohki, Y.; Tanifuji, K.; Yamada, N.; Imada, M.; Tajima, T.; Tatsumi, K. *Proc. Natl. Acad. Sci. U.S.A*. **2011**, *108* (31), 12635. doi:10.1073/pnas.1106472108.
(156) Ugulava, N. B.; Gibney, B. R.; Jarrett, J. T. *Biochemistry*, **2001**, *40* (28), 8343. doi:10.1021/bi0104625.